REAL-TIME MONITORING OF CONTACT BEHAVIOR OF RF MEMS SWITCHES WITH A VERY LOW POWER CMOS CAPACITIVE SENSOR INTERFACE

Adam Fruehling, Mohammad Abu Khater, Byunghoo Jung, Dimitrios Peroulis
Purdue University - Birck Nanotechnology Center, West Lafayette, IN, USA
fruehlin@purdue.edu, mabukhat@purdue.edu, jungb@purdue.edu, dperouli@purdue.edu

ABSTRACT

This paper presents the first ultra-low power, fully electronic methodology for real-time monitoring of the dynamic behavior of RF MEMS switches. The measurement is based on a capacitive readout circuit composed of 67 transistors with a 105 μm x 105 μm footprint consuming as little as 60 μW. This is achieved by accurately sensing the capacitance change around the contact region at sampling rates from 10 kHz to 5 MHz. Experimental and simulation results show that timing of not only the first contact event but also all subsequent contact bounces can be accurately measured with this technique without interfering with the switch performance. This demonstrates the potential of extending this technique to real-time on-chip dynamic monitoring of packaged RF MEMS switches through their entire lifetime and after their integration in the final system.

INTRODUCTION

Failure mechanisms related to the contact behavior of ohmic RF MEMS switches is still an active research topic. Contact degradation is typically observed as a change of switch contact resistance versus time that may lead to a permanently closed or permanently open state and represents a critical factor in their long term reliability [1]. Although contact resistance degradation is strongly coupled (among other factors) to contact force and bouncing events, no quantitative relationship exists today among them. Quantifying this coupling requires simultaneous real-time monitoring of the electrical and mechanical behavior. Recently Sumali et al. reported an attempt to do this by measuring a Sandia switch dynamic behavior through an optical interferometer [2]. While such optical techniques can provide very accurate real-time height and velocity information, they are inherently limited to unpackaged devices.

This paper presents, for the first time, a fully electronic methodology that enables the real-time monitoring of the dynamic behavior of packaged RF MEMS switches. The measurement is based on a capacitive readout interface circuit composed only of 67 transistors with a 105 μm x 105 μm footprint that consumes as little as 60 μW [3]. This is achieved by accurately sensing the capacitance change around the contact region at over sampling rates ranging from 10 kHz to 5 MHz or more. Sensing capacitance change, rather than absolute capacitance eliminates the adverse effects of parasitic capacitances and environmental factors. Timing and duration of all contact events can be accurately measured with this technique without interfering with the switch performance. Such electronic monitoring in real-time can provide important information on the contact force, adhesion force, and tip velocity that are critical for the understanding of the long-term failure mechanisms of packaged MEMS switches. The proposed method will eventually enable the integration of a small ultra-low power electronic circuit with the MEMS device which can monitor its performance even after the device is packaged and integrated into its final system.

RF MEMS SWITCH

A modified version of a previously reported [4] single-crystal-silicon (SCS) cantilever MEMS switch with gold-to-gold contacts is employed as a vehicle to demonstrate the methodology. SCS offers an ideal mechanical material for MEMS devices as it is nearly free of material defects and residual stress that may negatively affect the reliability and yield of typical MEMS switches based on thin-film metals. The critical modification here is the addition of a second sacrificial layer to the area of the bias structure in order to raise it higher than the contacts. This change carries several benefits. Chief among these, it increases the linear range of of motion such that the device is nearly in contact before the pull-in instability occurs. As a result, the beam is more capable to directly follow the input voltage waveform. It also increases the voltage overhead of the device before its silicon beam collapses so that the contact force can be increased

978-1-4244-5764-9/10/$26.00 ©2010 IEEE

substantially. A representative switch is shown in Figure 1. For scale, Figure 2 shows an image of the capacitive sensing circuit in appropriate relative size to the MEMS switch.

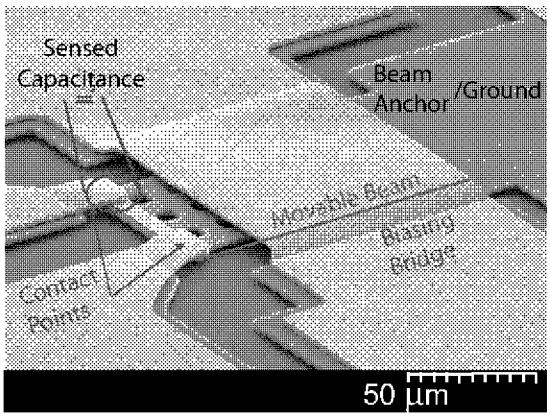

Figure 1: SEM image of representative single crystal silicon MEMS switch.

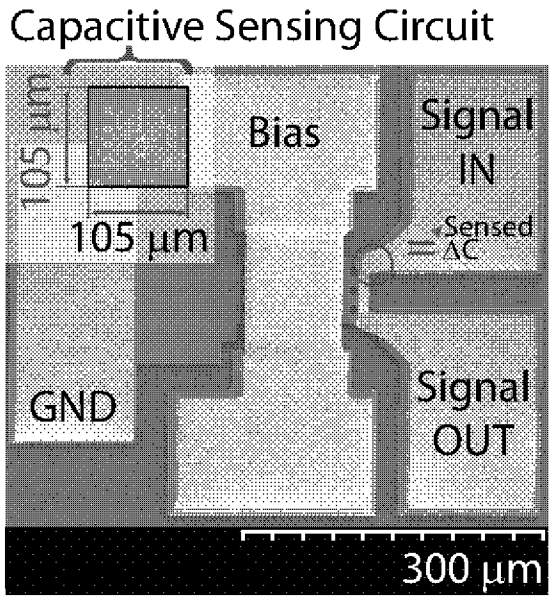

Figure 2: Image of the capacitive sensing circuit scaled to match the switch scale overlayed on an SEM of a representative switch.

CAPACITIVE READOUT CIRCUIT

The semi-digital readout circuit acts as capacitance to pulse-width-modulated signal (PWM) block [3]. The pulse width varies as a function of the RC time constant. The resistance is a fixed and known value, and the capacitance increases as the switch closes. As a result, the circuit is inherently linear. Due to the digital nature of the circuit, the output can be directly connected to a microprocessor to collect data in real-time.

Low power self-tuning comparators are used to compare the input voltage with the supply voltage, $V_{DD}/2$. As long as the voltage across the capacitance is less than this value, the output of the sensor interface circuit is high. The voltage across the capacitor (V_C) can be determined as shown in Equation 1 [5].

$$V_c = V_{DD}e^{-t/RC} \tag{1}$$

The time T required for V_C to reach $V_{DD}/2$, [5] can be found from Equation 2 [5].

$$V_C = \frac{V_{DD}}{2} = V_{DD}e^{-T/RC} \tag{2}$$

From Equation 2, T can be readily solved and is shown in Equation 3 [5].

$$T = RCln(2) \tag{3}$$

It can be seen that timing differences as measured by the circuit are linearly dependent on the measured capacitance changes. As such, the circuit's readout is independent of parasitic or reference capacitances. In order to eliminate any DC offset due to charge buildup over time, the transistor connected in parallel with the sensed capacitance is used to reset the voltage across the capacitor [3].

The maximum capacitance that can be read is limited by the clock high time (T_{HIGH}) and clock low time (T_{LOW}) [3]. Mathematically, this is represented in Equations 4 and 5 [3].

$$C_{MAX} = \frac{T_{HIGH}}{Rln(2)} \tag{4}$$

$$C_{MAX} = \frac{T_{LOW}}{5(r_{ON} \parallel R)} \tag{5}$$

Where r_{ON} is the transistor's on resistance. The factor 5 in Equation 5 is a result of requiring 5 time constants for the capacitor to be assumed to be completely discharged. The minimum of these two factors set the bottleneck for the maximum capacitance that can be measured. The minimum detectable capacitance is determined primarily by the jitter at the output [3]. The measured capacitances in this experiment are much greater than the circuit's threshold for minimum detectable capacitance.

Power consumption in the circuit was measured to be 60 μW with a reference resistance of 2.7 MΩ and a reference capacitance of 1 pF at an operating frequency of 32.768 kHz [3]. Power consumption was simulated in SPICE as shown in Figure 3 with a reference resistor of 100 kΩ to match the value used in the measurement of the MEMS bouncing. The operating frequency is determined by a clock

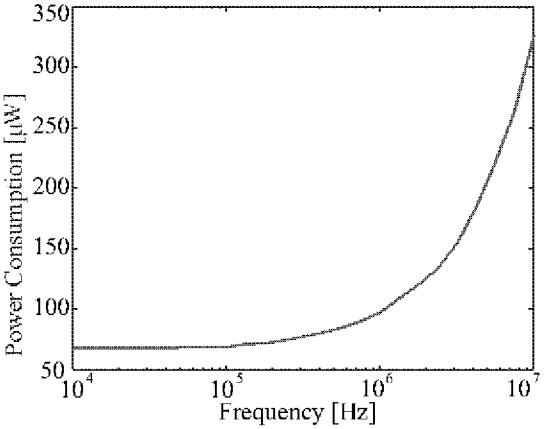

Figure 3: Cadence simulation of power consumption of the sensing circuit vs. frequency.

input. A crystal oscillator is commonly used to reduce jitter, though for experimental purposes a function generator was used in this work. While the power consumption of the clock source is non-negligible, in a system implementation it is often amortized across the entire system.

MODELING

To determine the post release dimensions needed for accurate modeling, a LEXT OLS-3100 confocal microscope [6] was used. The motion of the switch was modeled using Equation 6 [7]

$$m\frac{d^2x}{dt^2} + b\frac{dx}{dt} + kx = F_e + F_c \tag{6}$$

where m is the mass of the beam, b is the gas damping coefficient, and k is the spring constant of the beam, and F_e and F_c are the electrostatic force and contact forces respectively. The damping coefficient was estimated by using a mechanical quality factor of 18. The electrostatic force (F_e) is given by Equation 7 [7]

$$F_e = \frac{1}{2}\frac{\epsilon_0 V(t)^2}{(g_0 - x)^2} \tag{7}$$

where ϵ_0 is the free space permittivity, $V(t)$ is the applied voltage waveform, g_0 is the gap between the beam and the biasing bridge and x is the distance travelled by the tip of the beam. The contact force (F_c) is given by Equation 8 [7].

$$F_c = \frac{C_1 A}{(g_c - x)^3} - \frac{C_2 A}{(g_c - x)^{10}} \tag{8}$$

Here g_c is the gap between the beam tip and the contact pad. C_1 and C_2 are constants dependent on the adhesion and repulsive forces at the contact respectively and are chosen for simulation convergence [7].

EXPERIMENTS AND RESULTS

To obtain the electronic measurements, the device is connected to the circuit as shown in Figure 4. Figure 5 shows the raw output of the circuit and a biasing waveform synchronized in time. While the bias is at zero potential, the gap is at its maximum value and thus the capacitance at the contact in the off state is at its minimum value of approximately 1 fF. The resulting output pulse width is approximately 50% duty cycle. Upon actuation, as the beam moves toward the contact and the capacitance increases, resulting in an increase in the duty cycle until contact. This transition between low and high duty cycles occurs several times during a switching event as the beam bounces up repeatedly. When the beam settles in the closed state and remains in contact the duty cycle is constant at 80%. This value is a product of the crystal oscillator as the output duty cycle cannot exceed the clock duty cycle. The approximately 50% minimum duty cycle is due to the reading of parasitics of the circuit and setup.

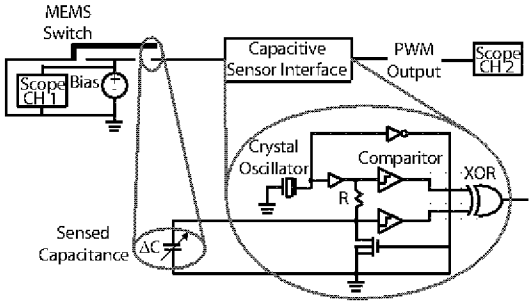

Figure 4: Experimental setup for measuring capacitance change of device in motion.

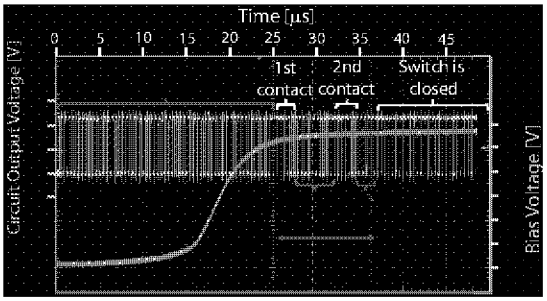

Figure 5: Oscilloscope capture of raw pulse-width modulated data and biasing for switch bouncing event with a synchronized time scale.

The switch landings predicted by the previously described simple 1-D model are overlayed with the measured contacts from the experiment in Figure 6. The bars represent the periods during which contact is made at the tip of the beam. It is worth

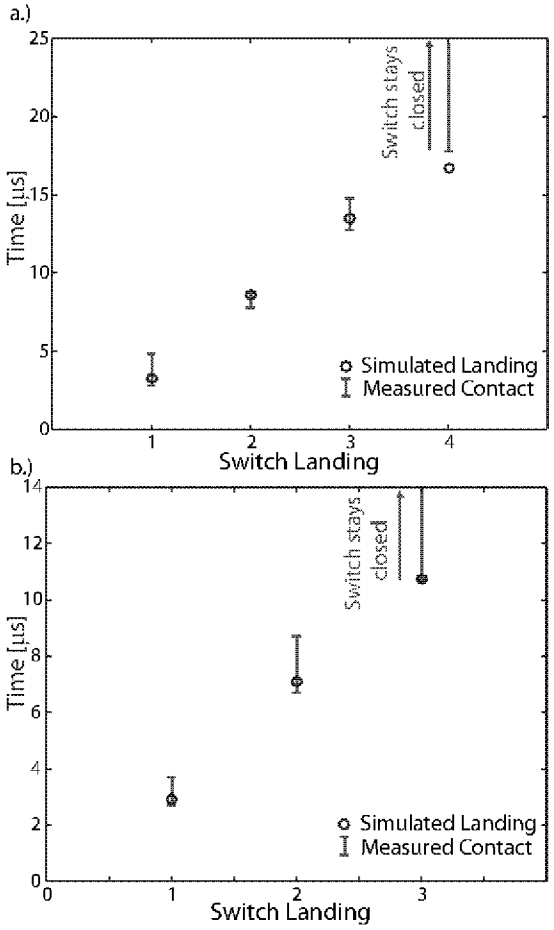

Figure 6: Simulated and measured switch bouncing at (a) 150 V and (b) 160 V biasing.

noting that even though the 1-D model employed accounts for an infinitesimally short contact duration, the measurement shows landings of finite duration in the μs range. All landings, however, correspond well with those predicted by the model even as the bias voltage is varied. This indicates that despite its limitations, the model is physically meaningful.

DISCUSSION AND CONCLUSION

There are certainly some weaknesses of the 1-D contact model used here. Foremost is the disagreement between the measured and simulated duration of contact events. The understanding of contact physics during dynamic events such as those examined here is an open question in literature and not fully captured in the model used. Additionally, employing optical techniques and refinement of this measurement technique to obtain height information will result in a greater insight into the dynamic behavior of this device and MEMS devices in general. Furthermore, the gas dynamics here are more complicated than can readily be employed in ANSYS by expecting constant and uniform damping during the duration of the event. Refinement of this technique to obtain dynamic height information, resistive information about the contact during these events, and refinement of the modeling techniques are areas of ongoing investigation.

This technique offers exciting possibilities for the real-time characterization of failure mechanisms of MEMS devices. Such a method could be used to develop an integrated failure prediction system and an adaptive closed-loop soft landing waveform for packaged MEMS switches. The size and power consumption of the circuit as well as its simple output makes it an ideal candidate for integration with packaged MEMS devices for in situ health monitoring.

ACKNOWLEDGEMENT

This work has been supported by the Defense Advanced Research Projects Agency under the IMPACT Program grant Number 2006-05822-06 and the Defence Treat Reduction Agency grant Number HDTRA-08-1-0026.

References

[1] S. Patton, J. Zabinski, "Fundamental studies of Au contacts in MEMS RF switches", Tribology Letters, vol. 18, no. 2, February 2005, pp. 215-230

[2] H. Sumali, J. Massad, D. Czaplewski, C. Dyck, "Waveform design for pulse-and-hold electrostatic actuation in MEMS", Sensors and Actuators A, April 2006, pp. 213-220

[3] J. Lu, M. Inerowicz, S. Joo, J-k. Kwon, B. Jung, "A Low-Power, Wide-dynamic range Semi-Dgital Universal Sensor Readout Circuit Using Pulse-Width Modulation", 2009, submitted to IEEE Sensors Journal

[4] A. Fruehling, R. Pimpinella, R. Nordin, D. Peroulis,"A Single-crystal Silicon DC-40 GHz RF MEMS Switch", IEEE MTT-S, June 2009, pp. 1633-1636

[5] M. Abu Khater, Master's Thesis, Purdue University, August 2009

[6] Olympus America Industrial Microscopy: http://www.olympusamerica.com/seg_industrial/product.asp?product=1012

[7] G. Rebeiz, "RF MEMS Theory, Design, and Technology" *John Wiley and Sons*, 2003.